Phase Relations Associated with One-Dimensional Shell Effects in Thin Metal Films

T. Miller,[1,2] M. Y. Chou,[3] and T.-C. Chiang[1,2,*]

[1]*Department of Physics, University of Illinois at Urbana-Champaign, 1110 West Green Street, Urbana, Illinois 61801-3080, USA*
[2]*Frederick Seitz Materials Research Laboratory, University of Illinois at Urbana-Champaign, 104 South Goodwin Avenue, Urbana, Illinois 61801-2902, USA*
[3]*School of Physics, Georgia Institute of Technology, Atlanta, Georgia 30332-0430, USA*

(Received 24 January 2009; published 11 June 2009)

The physical and chemical properties of thin metal films show damped oscillations as a function of film thickness (one-dimensional shell effects). While the oscillation period, determined by subband crossings of the Fermi level, is the same for all properties, the phases can be different. Specifically, oscillations in the work function and surface energy are offset by 1/4 of a period. For Pb(111) films, this offset is ~0.18 monolayers, a seemingly very small effect. However, aliasing caused by the discrete atomic layer structure leads to striking out-of-phase beating patterns displayed by these two quantities.

DOI: 10.1103/PhysRevLett.102.236803 PACS numbers: 73.21.Fg, 73.20.At, 79.60.Dp

The periodic property variations of the elements in the periodic table can be understood in terms of electrons filling successive atomic shells for increasing atomic number Z. A similar periodicity occurs in thin films, in which the electrons in films of increasing thicknesses fill the subbands arising from confinement and quantization along the direction perpendicular to the film surface [1]. Such periodic variations have been observed in the thermal stability [2], surface energy [3], work function [4], chemisorption behavior [5], film growth behavior [3,6], electron-phonon coupling [7], and superconducting transition temperature [8–10] in a number of systems. While these properties of a given system all vary with the same period, the oscillation phases can differ. These phase relations, largely neglected up to now, are of basic importance to nanoscale phenomena and property tuning in thin film systems.

Specifically, first-principles calculations of the surface energy and work function of Pb(111) films [11] have shown beating patterns that are out of phase, a very puzzling result. We derive herein a general phase rule: The oscillations in surface energy lead the oscillations in work function by 1/4 of a period. For Pb(111), this phase shift corresponds to 0.18 monolayers (ML). While this is much less than an atomic layer, it is by no means negligible. In fact, aliasing [12,13] caused by the discrete atomic layer structure of the films substantially accentuates the effect, resulting in large differences in the beating patterns. A second example of this phase relationship is seen in experimental results for Ag(100) films grown on Fe(100) [4,7]. The oscillation period is ~5.7 ML, much larger than the Pb(111) case. Such a long oscillation period does not yield recognizable beating patterns. Yet the phase shift between the surface energy and work function, ~1.4 ML, is large enough for direct observation. In the following, we provide an analytic derivation and numerical examples for the phase relations and the beating functions in terms of subband crossings of the Fermi level.

Figure 1 shows the results of first-principles calculations of E_S (surface energy per surface atom) and W (work function) of freestanding Pb(111) films of thicknesses N ranging from 1 to 25 ML [11]. Both quantities vary with an approximately bilayer period (even-odd oscillations). A slight departure from exact bilayer periodicity results in a beating pattern, as the even-odd oscillations undergo a phase reversal over a beating period of ~9 ML. The envelope functions of the beating patterns are indicated (discussed below). The two vertical dashed lines mark the

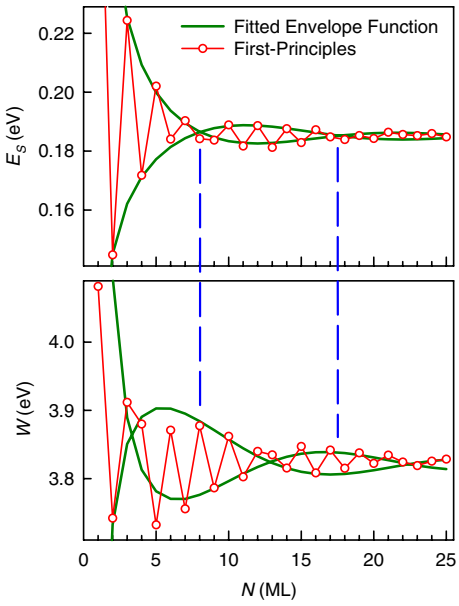

FIG. 1 (color online). Surface energy E_S per surface atom and work function W as a function of thickness N of freestanding Pb(111) films from a first-principles calculation (results taken from [11]). Also shown are envelope functions derived from a model fit to highlight the beating patterns. The two vertical lines are lined up with two adjacent nodes in E_S and highlight the out-of-phase relationship between the envelope functions of E_S and W.

nodes in the envelope functions of E_S, each of which lines up with an antinode in the envelope functions of W. The beating patterns for the two cases are clearly out of phase.

Our derivation is based on the standard quantum well model [14–21] with the quantization condition

$$2k_n h + 2\phi = 2(n-1)\pi, \tag{1}$$

where k is the wave vector, h is the width of the quantum well, ϕ is the electron phase shift at each boundary (assuming a symmetric well), and $n = 1, 2, 3\ldots$ is a quantum number. Here the film thickness h is allowed to vary continuously, yielding details that are otherwise lost in calculations based on discrete atomic layers. The minimum of the nth subband has energy

$$E_n = \frac{\hbar^2 k_n^2}{2m}. \tag{2}$$

A straightforward derivation yields the density of states per unit volume at the chemical potential $D(\mu)$, the chemical potential (or Fermi level) μ, and the surface energy per unit area E_S:

$$D(\mu) = \frac{1}{2\pi}\frac{2m}{\hbar^2}\frac{n_0}{h}, \tag{3}$$

$$\mu = \frac{\rho}{D(\mu)} + \langle E_n \rangle, \tag{4}$$

$$E_S = \frac{1}{8\pi}\frac{2m}{\hbar^2} n_0(\mu^2 - \langle E_n^2 \rangle) - \frac{3}{10}\rho h \mu_\infty, \tag{5}$$

where n_0 is the quantum number of the highest nonempty subband, $\langle \ldots \rangle$ denotes averaging over nonempty subbands, μ_∞ is the bulk chemical potential, and ρ is the electron density. From Eq. (1), successive subband crossings of the Fermi level occur at a film thickness increment of

$$\Delta h = \frac{\pi}{k_F}, \tag{6}$$

where k_F is the Fermi wave vector. Thus, all properties vary with the period Δh, which equals one-half of the Fermi wave length.

Standard thermodynamic arguments show that E_S is a smooth function of h, while μ and p (pressure), related to the partial derivatives of the total energy, are continuous but not necessarily smooth. From Eqs. (1) and (2), one can deduce

$$\frac{dE_n}{dh} = -\frac{2E_n}{h} + O\left(\frac{1}{h^2}\right). \tag{7}$$

The high-order correction can be ignored for all practical purposes. From Eqs. (3)–(5), one can derive the following central equations:

$$\frac{1}{h^2}\frac{d}{dh}(h^2\mu) = 6\pi\frac{\hbar^2}{2m}\frac{\rho}{n_0} = \frac{3\rho}{hD(\mu)}, \tag{8}$$

$$\frac{1}{h^4}\frac{d}{dh}(h^4 E_S) = \frac{3}{2}\rho(\mu - \mu_\infty). \tag{9}$$

Physically, the rate of change of the chemical potential for increasing h, or increasing electron filling, is related to the inverse of the density of states at the chemical potential, and the rate of change of the surface energy is related to the chemical potential, the energy required to add an electron. $D(\mu)$ is related to the in-plane conductance [22], superconductivity [23], and chemisorption properties [5] of thin films.

The results from a numerical calculation are shown in Fig. 2, using nominal parameter values appropriate for Pb(111) within a free electron approximation [24]. The top panel shows the evolution of the quantized electron structure E_n. The subbands cross μ with a period of $\Delta N = 0.7$ ML; the crossings are marked by the vertical dashed lines. The second panel shows $D(\mu)$. Each subband has a constant density of states, and the total density of states is a series of steps [22]. Upon normalizing by the volume to yield $D(\mu)$, it becomes a series of diminishing sawteeth. Its inverse $D(\mu)^{-1}$ is presented in the third panel. The next panel displays the work function relative to the bulk limit: $\Delta W = -\Delta\mu \equiv \mu_\infty - \mu$. The series of cusps [25] arise from a weighted integration of the sawteeth in $D(\mu)^{-1}$ per Eq. (8). The bottom panel displays ΔE_S, the surface energy

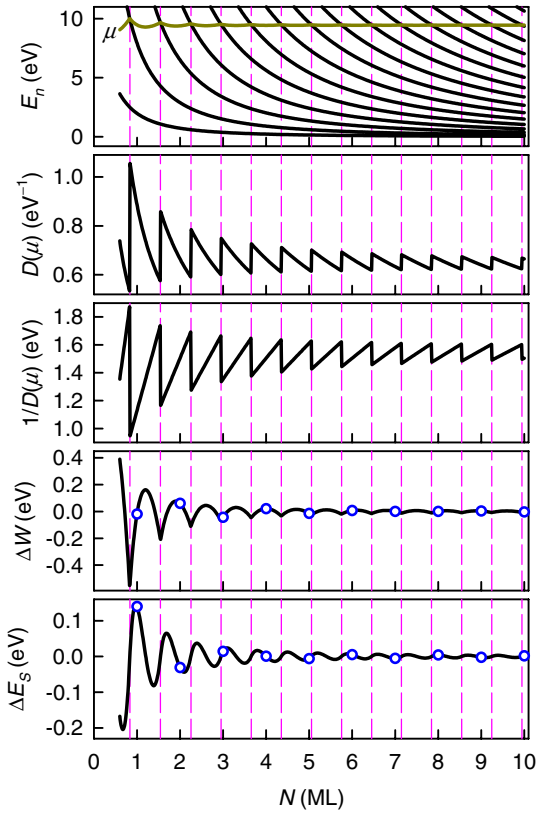

FIG. 2 (color online). Results from a quantum well model calculation (partly reproduced from or based on [3]). From top to bottom: the quantized electronic structure and the chemical potential μ, the density of states per atom at the chemical potential, the inverse of the density of states, the work function relative to the bulk limit, and the surface energy per surface atom relative to the bulk limit. Subband crossings are marked by vertical dashed lines. The values of ΔE_S and ΔW at integer N's are indicated by circles.

relative to the bulk limit. It is a weighted integration of $\Delta\mu = -\Delta W$ per Eq. (9); the result can be well represented by a smooth damped sinusoidal function. Equation (9) also shows that each cusp in ΔW (local minimum) corresponds to a point of maximum positive slope in E_S. Thus, the oscillation maxima in E_S lead the maxima in ΔW by 1/4 of a period, or ~0.18 ML for Pb(111).

As discussed above, ΔE_S can be modeled by a damped sinusoidal function

$$\Delta E_S = \frac{A\sin(2k_F h + \Phi) + C}{h^\alpha}, \tag{10}$$

where $k_F = 1.58$ Å^{-1}, the free electron value, corresponds to an oscillation period of $\Delta N = 0.7$ ML. This period, less than one atomic layer, cannot be detected readily for real films where N takes on integer values only. The values of ΔE_S and ΔW at integer N's are indicated by the circles in Fig. 2. These discrete values are replotted in Fig. 3; the apparent oscillations are governed by a Fermi wave vector measured from the zone boundary $k_F' = k_F - \pi/t$, where t is the monolayer thickness. Mathematically, replacing k_F in Eq. (10) by k_F' retains the functional values of ΔE_S at integer values of N. With $k_F' = 0.49$ Å^{-1}, the oscillation period is $\Delta N = 2.2$ ML, and the results in Fig. 3 indeed show approximate bilayer, or even-odd, oscillations. The slight departure of the period from 2 ML results in a beating pattern governed by the difference wave vector $k_E = \pi/(2t) - k_F' = 0.07$ Å^{-1}. This beating modulation becomes evident with the transformation:

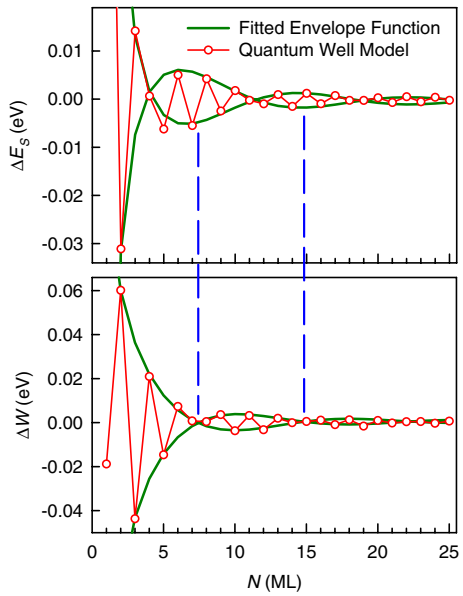

FIG. 3 (color online). Results from a quantum well model calculation for ΔE_S (surface energy per surface atom relative to the bulk limit) and ΔW (work function relative to the bulk limit) for integer film thicknesses N (partly reproduced from or based on [3]). Also shown are envelope functions derived from a model fit. The two vertical lines are lined up with two adjacent nodes in ΔW.

$$\Delta E_S = \frac{A\sin(2k_F' Nt + \Phi) + C}{(Nt)^\alpha} = \frac{A(-1)^{N+1}\sin(2k_E Nt - \Phi) + C}{(Nt)^\alpha}. \tag{11}$$

The factor $(-1)^{N+1}$ gives rise to the even-odd oscillations; replacing it with ± 1 yields the envelope functions

$$\frac{\pm A\sin(2k_E Nt - \Phi) + C}{(Nt)^\alpha}. \tag{12}$$

A fit of the results in Fig. 3 using Eq. (12) is shown. The same analysis for the first-principles results yields the envelope functions in Fig. 1. Other choices of the Fermi wave vector are possible [26].

The beating patterns of ΔE_S and ΔW in Fig. 3 are mutually out of phase, the same as that seen in Fig. 1. The reason is that Φ in Eq. (10) differs by $\pi/2$ (1/4 of a period) for these two cases [27]. This phase difference is preserved for the transformations from k_F to k_F' and to k_E. Since the period is much larger for the beating pattern, the phase difference becomes much more apparent. The patterns in Fig. 3 are somewhat different from those in Fig. 1. Specifically, the internode distance in Fig. 3 is ~7 ML, rather than ~9 ML as in Fig. 1. The discrepancy is caused by a slight difference (<1%) between the free electron Fermi wave vector used in the model calculation and the actual value for Pb(111). The envelope function is thus a highly sensitive measure of minute details in the electronic structure of the system.

Another case of interest is Ag films on Fe(100). Figure 4 shows the quantized electronic structure, where the periodicity of Fermi level crossings is $\Delta N = 5.7$ ML (top panel) [14]. Beating effects are not apparent for this long period. However, a phase difference of $5.7/4 = 1.4$ ML is expected between the work function and surface energy. The middle panel shows the work function [4], which exhibits downward cusps at the crossings (near $N = 4$ and 10) as indicated by the vertical dashed lines. The bottom panel shows the maximum thermal stability temperature determined by experiment [2]. The most stable thickness at $N = 5$ should correspond to a deep minimum in surface energy. Based on an inspection of Fig. 2, one might expect the minimum surface energy to occur at $N = 4 - 1.4 = 2.6$ ML, but it is actually at $N = 4 + 1.4 \approx 5$ ML. The reason for the sign reversal is that the 5.7 ML period actually corresponds to a Fermi wave vector measured from the zone boundary $k_F' = \pi/t - k_F$ [14]. The sense of the Fermi wave vector is thus reversed, and so the sign of the phase difference is reversed. This reversal is also evident from the top panel in Fig. 4, where each E_n increases for increasing N (or decreasing k), which is opposite to what is seen in Fig. 2.

A key conclusion of this work is that the phases of oscillations associated with one-dimensional shell effects in films depend on the properties of interest. Specifically, the work function exhibits downward cusps at subband

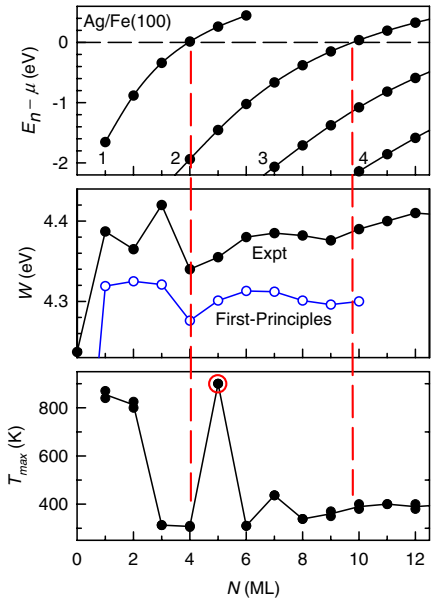

FIG. 4 (color online). Results for Ag films on Fe(100) (taken from [2,4]). From top to bottom: the quantized electronic structure, the work function, and the maximum thermal stability temperature $T_{\max}$. The two vertical dashed lines mark subband crossings. The highest stability temperature at $N = 5$, marked by a circle, represents a lower bound.

crossings, while the surface energy has maximum positive slopes; thus, the maxima in E_S lead in phase by $1/4$ of a period compared to the maxima in W. The density of states at the Fermi level shows sharp jumps at the crossings. This should affect the superconducting transition temperature, but the actual oscillation phase of the transition temperature can be affected by electron-phonon coupling that depends on the details of the wave functions. In-plane conduction in the normal state is, however, expected to be synchronous with the oscillations of the density of states. Chemisorption properties are also likely to be synchronous; however, the phases can differ if the adsorbates have little density of states around the substrate chemical potential.

This work is supported by the U.S. Department of Energy (Grant No. DE-FG02-07ER46383 for T.-C. C. and Grant No. DE-FG02-97ER45632 for M. Y. C.). We acknowledge the ACS Petroleum Research Fund and the U.S. National Science Foundation (Grant No. DMR-05-03323) for partial support of the equipment and personnel at the Synchrotron Radiation Center (SRC). The SRC is supported by the U.S. National Science Foundation (Grant No. DMR-05-37588). We acknowledge helpful discussions with C. Ken Shih.

*Corresponding author.
tcchiang@illinois.edu

[1] T.-C. Chiang, Science **306**, 1900 (2004).
[2] D.-A. Luh, T. Miller, J. J. Paggel, M. Y. Chou, and T.-C. Chiang, Science **292**, 1131 (2001).
[3] P. Czoschke, L. Basile, Hawoong Hong, and T.-C. Chiang, Phys. Rev. Lett. **93**, 036103 (2004); Phys. Rev. B **72**, 075402 (2005).
[4] J. J. Paggel, C. M. Wei, M. Y. Chou, D.-A. Luh, T. Miller, and T.-C. Chiang, Phys. Rev. B **66**, 233403 (2002).
[5] X. Ma *et al.*, Proc. Natl. Acad. Sci. U.S.A. **104**, 9204 (2007).
[6] M. C. Tringides, M. Jalochowski, and E. Bauer, Phys. Today **60**, No. 4, 50 (2007).
[7] D.-A. Luh, T. Miller, J. J. Paggel, and T.-C. Chiang, Phys. Rev. Lett. **88**, 256802 (2002).
[8] Y. Guo *et al.*, Science **306**, 1915 (2004).
[9] M. M. Özer, Y. Jia, Z. Zhang, J. R. Thompson, and H. H. Weitering, Science **316**, 1594 (2007).
[10] D. Eom, S. Qin, M.-Y. Chou, and C. K. Shih, Phys. Rev. Lett. **96**, 027005 (2006).
[11] C. M. Wei and M. Y. Chou, Phys. Rev. B **68**, 125406 (2003).
[12] F. J. Harris, *Multirate Signal Processing for Communication Systems* (Prentice-Hall, Englewood Cliffs, NJ, 2004).
[13] W. H. Press, S. A. Teukolsky, W. T. Vetterling, and B. P. Flannery, *Numerical Recipes in Fortran* (Cambridge University Press, Cambridge, England, 1992), 2nd ed.
[14] T.-C. Chiang, Surf. Sci. Rep. **39**, 181 (2000).
[15] F. J. Himpsel, J. E. Ortega, G. J. Mankey, and R. F. Willis, Adv. Phys. **47**, 511 (1998).
[16] S.-Å. Lindgren and L. Walldén, in *Electronic Structure*, Handbook of Surface Science Vol. 2, edited by S. Holloway, N. V. Richardson, K. Horn, and M. Scheffler (Elsevier, Amsterdam, 2000).
[17] M. Milun, P. Pervan, and D. P. Woodruff, Rep. Prog. Phys. **65**, 99 (2002).
[18] L. Aballe, C. Rogero, P. Kratzer, S. Gokhale, and K. Horn, Phys. Rev. Lett. **87**, 156801 (2001).
[19] I. Matsuda, T. Ohta, and H. W. Yeom, Phys. Rev. B **65**, 085327 (2002).
[20] A. Mans, J. H. Dil, A. R. H. F. Ettema, and H. H. Weitering, Phys. Rev. B **66**, 195410 (2002).
[21] Y. Z. Wu, C. Y. Won, E. Rotenberg, H. W. Zhao, F. Toyoma, N. V. Smith, and Z. Q. Qiu, Phys. Rev. B **66**, 245418 (2002).
[22] N. Trivedi and N. W. Ashcroft, Phys. Rev. B **38**, 12 298 (1988).
[23] J. M. Blatt and C. J. Thompson, Phys. Rev. Lett. **10**, 332 (1963).
[24] We employ an infinite-well model with the well width adjusted to account for charge spillage. The charge spillage parameter is chosen to null out the electric field at the center of the films to minimize the electrostatic energy. See Ref. [3] for details.
[25] F. K. Schulte, Surf. Sci. **55**, 427 (1976).
[26] Another possible choice of the Fermi wave vector is $k_F'' = 2\pi/t - k_F$, which is equivalent to measuring the Fermi surface from the zone center in the reduced zone. This choice leads to an oscillation period of 1.8 ML.
[27] For the surface energy, $\Phi = 2\phi_F$, where ϕ_F is the phase shift in Eq. (1) evaluated at the Fermi level. For the work function, $\Phi = 2\phi_F - \pi/2$.